

Titre: Workpiece subsurface temperature study during aluminum skin
Title: milling in slotting and ramping

Auteurs: Xavier Rimpault, Alexandre Il, Jean-François Chatelain, Jean-François
Authors: Lalonde, & Marek Balazinski

Date: 2018

Type: Article de revue / Article

Référence: Rimpault, X., Il, A., Chatelain, J.-F., Lalonde, J.-F., & Balazinski, M. (2018).
Citation: Workpiece subsurface temperature study during aluminum skin milling in slotting
and ramping. Procedia CIRP, 77, 417-420.
<https://doi.org/10.1016/j.procir.2018.08.295>

Document en libre accès dans PolyPublie

Open Access document in PolyPublie

URL de PolyPublie:
PolyPublie URL: <https://publications.polymtl.ca/5115/>

Version: Version officielle de l'éditeur / Published version
Révisé par les pairs / Refereed

Conditions d'utilisation:
Terms of Use: CC BY-NC-ND

Document publié chez l'éditeur officiel

Document issued by the official publisher

Titre de la revue: Procedia CIRP (vol. 77)
Journal Title:

Maison d'édition: Elsevier
Publisher:

URL officiel: <https://doi.org/10.1016/j.procir.2018.08.295>
Official URL:

Mention légale: © 2018 The Authors. Published by Elsevier Ltd. This is an open access article under the
Legal notice: CC BY-NC-ND license (<http://creativecommons.org/licenses/by-nc-nd/3.0/>)

8th CIRP Conference on High Performance Cutting (HPC 2018)

Workpiece subsurface temperature study during aluminum skin milling in slotting and ramping

Xavier Rimpault^{a,b,*}, Alexandre Ilia^{a,c}, Jean-François Chatelain^a, Jean-François Lalonde^c,
Marek Balazinski^b

^aDepartment of Mechanical Engineering, École de technologie supérieure (ÉTS), Montréal, QC H3C 1K3, Canada

^bDepartment of Mechanical Engineering, Polytechnique Montréal, Montréal, QC H3T 1J4, Canada

^cBombardier Aerospace, Saint-Laurent, QC H4R 1K2, Canada

* Corresponding author. Tel.: +1-514-396-8800; fax: +1-514-396-8530. E-mail address: xavier.rimpault@polymtl.ca

Abstract

Aluminum alloys are widely used in the industry such as aerospace. This study was motivated by the replacement of the chemical milling of thin aluminum parts with mechanical milling. To remain within requirements of design specifications, this process needs to be tuned and optimized using e.g. cutting forces, vibrations and surface integrity assessments. In aerospace industry, the temperature control is indeed a major issue since the heat generated and transferred to the workpiece during machining can affect the surface integrity and thus the component properties. A heat analysis is ultimately needed to optimize, control and certify a milling process.

In this research, embedded thermocouples at specific locations in a 2024-T3 aluminum thin plate subsurface have been used to evaluate local temperatures during machining. Two milling operations have been selected: slotting and ramping. The measurement data showed workpiece temperature increase with the feed reduction. An increase of the internal-temperature is indicated while the cutting tool moves into workpiece from the beginning of the cutting stage to the middle line of the tool-path. Finally, the test results shown that the effect of the feed (both radial and axial) has one of the most significant influence on subsurface accumulated heat, more than the cutting speed.

© 2018 The Authors. Published by Elsevier Ltd.

This is an open access article under the CC BY-NC-ND license (<https://creativecommons.org/licenses/by-nc-nd/4.0/>)

Selection and peer-review under responsibility of the International Scientific Committee of the 8th CIRP Conference on High Performance Cutting (HPC 2018).

Keywords: Aluminium; Cutting temperature; Thermocouple; Slotting; Ramping

1. Introduction

Due to struggle to manufacture lighter and greener aircraft, the aerospace industry widely uses aluminium alloys and pushes it into thin wall/web frames and skins amongst other parts. Such structural parts as skins are very sensitive to clamping, cutting forces and cutting temperatures because of their weak stiffness and rigidity design [1].

To avoid those problems, chemical machining was preferred so far in the industry. However, with the green policy enforced by aerospace companies, mechanical milling is developed to replace a highly polluting chemical process. In addition to the environmental footprint reduction, the use of mechanical

milling allows to reduce cost and improve the process efficiency. Nevertheless, due to the concurrent action of friction and shearing during cutting, the heat is generated in the cutting area: at the tool-workpiece interface and tool-chip interface. Some of this heat diffuses into the workpiece. The high temperature in the workpiece subsurface leads to residual stresses once the heat is dissipated. Both tensile stresses (mostly thermally caused) and compression stresses (mostly mechanically caused) are source of residual stresses in the part after machining. The combination of residual stresses and thin walls, in the part design, may lead to part distortions and a lower fatigue resistance.

Due to the intermittent nature of the milling process, tool cutting edges might have to support considerable temperature variations [2]. The heat generated by this transient phenomenon is associated with metallurgical transformation [3], which affects the machining performance. Using cutting fluids or heat-pipe assisting cooling [4] is a solution to control cutting temperature and prevent extensive tool wear [5].

Regarding the process itself, the temperature was found higher in cases with high cutting speed and low feed [3]. The heat generated whether in conventional or high-speed milling is too abrupt and high to be flown through the workpiece [6]. The heat, in addition to cyclic mechanical loads onto the tool, downgrades the tool life but it also affects the surface integrity of the machined workpiece [4] [5] [7]. The sub-surface material properties are then affected and modified due to the combined action of thermal and mechanical stresses and possible phase transformation, which will define the residual stresses distribution afterwards [8]. Those factors through cutting parameters, cutting conditions and tool path need to be considered in order to control and reduce the residual stresses.

Therein, the subsurface temperature assessment was performed with different cutting parameters in ramping and slotting in order to evaluate the impact on the ramping tool path on the workpiece temperature in comparison with the slotting.

2. Materials and methodology

2.1. Machining setup

Wrought 2024-T3 aluminum alloy plates of 2.54 mm thick were machined using a 3-axis milling center with a worktable equipped with a vacuum system to fix the workpiece. The workpiece plate was clamped on the table through Medium Density Fibreboard. This allows to distribute the vacuum force over the whole table top surface, avoiding thus any additional clamping system.

The end-mill selected is a diamond-like carbon (DLC) coated carbide tool with four flutes and a diameter of 19.05 mm. Each flute has a 12° cutting edge rake angle. The tool tip has a 3.96 mm corner radius. A single tool was used in down-milling for all experiments and very low tool wear has been observed during the tests. The cutting conditions selected based on a Taguchi plan and add-ons are introduced in Fig. 1 and in Table 1. Nine sets of cutting parameters are planned with Taguchi which five sets are repeated. Four additional intermediate sets of cutting parameters were chosen to validate results [9].

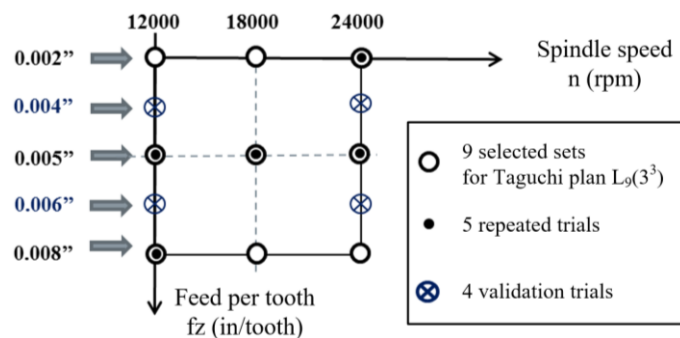


Fig. 1. Design of experiments for the cutting parameters selection

Table 1. Plan of experiments

Tests	Feed per tooth fz (in/tooth)		Spindle speed n (rpm)		Cutting speed Vc – ft/min (m/min)	Plunging ramping angle	
	Levels					Levels	
1	1	0.002’’	1	12000	2356 ft/min (718 m/min)	1	7°
2*		0.004’’	*	12000			5°
3	2	0.005’’	1	12000		2	5°
3bis	2	0.005’’	1	12000			
4*		0.006’’		12000			3°
5	3	0.008’’	1	12000		3	3°
5bis	3	0.008’’	1	12000			
6	1	0.002’’	2	18000	3534 ft/min (1077 m/min)	2	5°
7	2	0.005’’	2	18000		3	3°
7bis	2	0.005’’	2	18000			
8	3	0.008’’	2	18000		1	7°
9	1	0.002’’	3	24000	4712 ft/min (1436 m/min)	3	3°
9bis	1	0.002’’	3	24000			
10*		0.004’’		24000			3°
11	2	0.005’’	3	24000		1	7°
11bis	2	0.005’’	3	24000			
12*		0.006’’		24000			5°
13	3	0.008’’	3	24000		2	5°

*: Four additional tests for inter level factor validation / bis: Repeated tests without measurement at the end of the ramping motion

2.2. Temperature measurement

Due to the low radiation characteristics of the workpiece material, temperature was recorded using embedded thermocouples. Those embedded thermocouples allow to measure machined sub-surface temperature [3] [10]. Thus, they were used to evaluate the workpiece subsurface temperature distributions during the milling tests. K-type thermocouples of 80 µm diameter were chosen for their quick response of less than 20 ms. Small holes (0.79 mm) were drilled along the tool paths in order to insert the thermocouples within. To prevent heat flow alteration between thermocouples and the workpiece, hot junctions were welded without metal addition.

Fig. 2 shows the thermocouples position in the plate. The hole depth and so the in-thickness plate position of the thermocouple was evaluated to be as close as possible to the machined surface. The holes were then filled with thermal cement (Omega OB-400 cement with 62.46 W/°C.m² of thermal conductivity) to ensure the securely maintain the thermocouples in position and allow proper heat transfer from the aluminum plate to the hot junction.

Thermocouples were wired to a National instrument (Ni9213) acquisition system that allowed to simultaneously record 16 temperature positions sampled at 100 Hz/channel.

For this study, the subsurface temperature was mapped using thermocouples positioned at the same depth within the material (1.3 mm below the machined surface). For each experiment, five thermocouples were embedded within the plate (Fig. 3). The first one is located beneath the machined surface at the end of the ramping motion and centered with respect to the tool path (named Tramp). Two additional thermocouples are located

under the machined surface in the middle of the tool path (T12 and T22). T22 allows to observe the effect of the feed deceleration due to the change in the tool path direction. These locations are usually the source of hot spots.

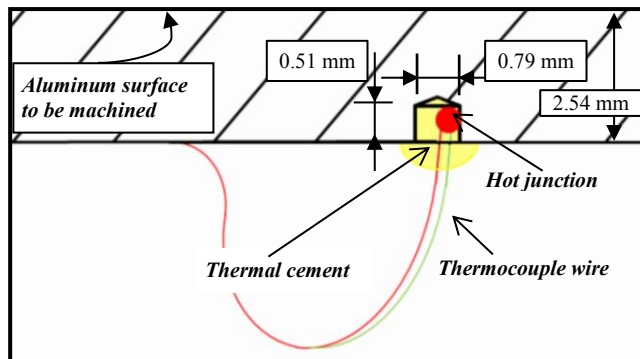


Fig. 2. Thermocouple embedded within the aluminium plate

Finally, the last thermocouples (T11 and T13) are located on each side of the middle line as shown in Fig. 4. This allows to have a good overview of the temperature distribution without deviation due to hot spots. The difference in the chip thickness can influence the heat generated during cutting and some heat diffused into the workpiece. For example, T13 and T12 temperature comparisons could highlight those variations.

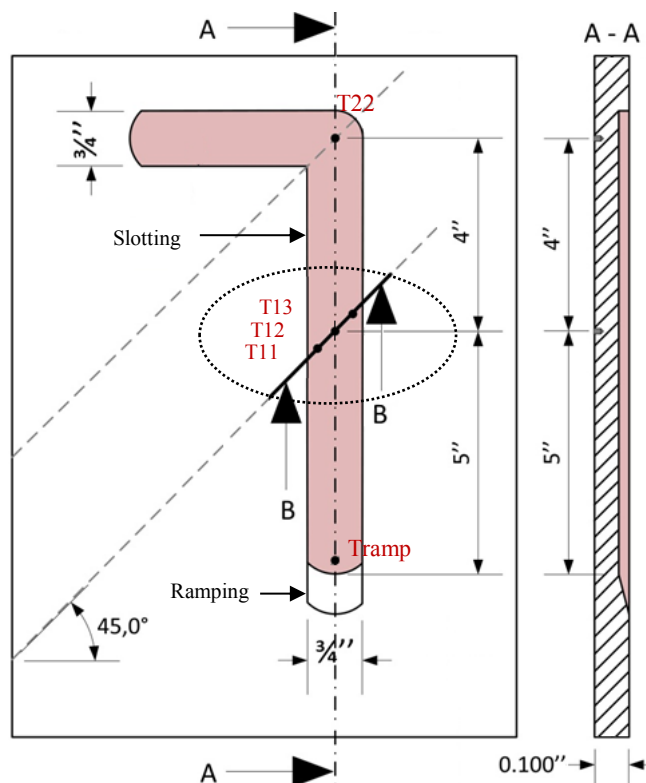


Fig. 3. Thermocouples placement grid

The experiments focused exclusively on the diving of the tool observed at the end of the ramping motion, and slotting. For all measurements, the thermocouples are below the median line, 0.187" from the end of ramping edge.

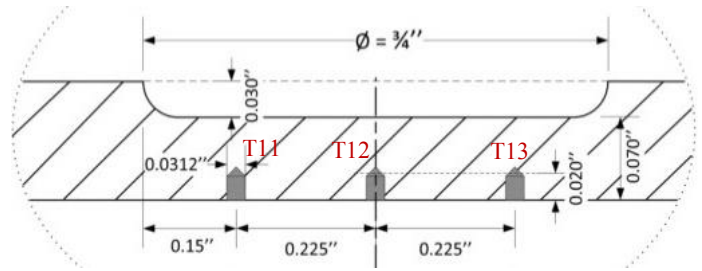


Fig. 4. T11, T12 and T13 thermocouples in the section view B-B OF Fig. 3

3. Results and discussion

Table 2 shows the measurement results of the temperature for the heat transferred into the workpiece at the end of the ramping motion (Tramp) and during the slotting motion for the cutting parameters selected in the design of experiments.

As observed in the literature, results herein show that higher cutting speed and higher feed per tooth leads to lower heat transfer into the workpiece. The feed variations seems to have a greater impact on the temperature measured in the workpiece subsurface.

Table 2. Temperatures recorded in the workpiece subsurface at ramping (Tramp) and during slotting

Tests	Measured maximum local temperatures			
	At ramping Tramp (°C)	during slotting		
		T12 (°C)	T13 (°C)	T22 (°C)
1	76.18	66.22	55.86	57.24
2*	64.93	48.27	45.99	50.06
3	61.15	42.16	42.54	46.32
3bis	-	43.78	41.18	44.29
4*	56.61	37.88	40.85	46.45
5	52.85	40.90	39.30	41.35
5bis	-	38.54	36.85	43.36
6	79.95	54.43	55.46	58.59
7	51.72	37.23	38.20	44.03
7bis	-	37.43	38.07	43.42
8	40.70	44.74	38.24	41.46
9	78.05	52.53	49.14	48.66
9bis	-	49.39	52.79	48.11
10*	58.29	43.40	36.73	45.48
11	43.08	39.76	38.23	42.85
11bis	-	38.24	38.28	39.57
12*	42.67	35.41	35.59	40.32
13	40.35	34.43	34.40	43.10

The temperature variations measured between T12 and T22 are between -13% (test 1) and +25% (test 13) (Table 2). The tool deceleration at the T22 location is probably the cause of this difference. A high feed per tooth leads to relatively higher temperature gap between T22 and T12.

Fig. 5 depicts the difference between Tramp temperatures and T12. The observed temperature Tramp, notably higher than those measured at the T12 location, is not only caused by a variation of the feed per tooth but rather by the presence of an axial force (axial federate per tooth). Tramp is 10% to 50% higher than temperatures observed in T12 (if test 8 Tramp is not considered because it might be an experimental outlier).

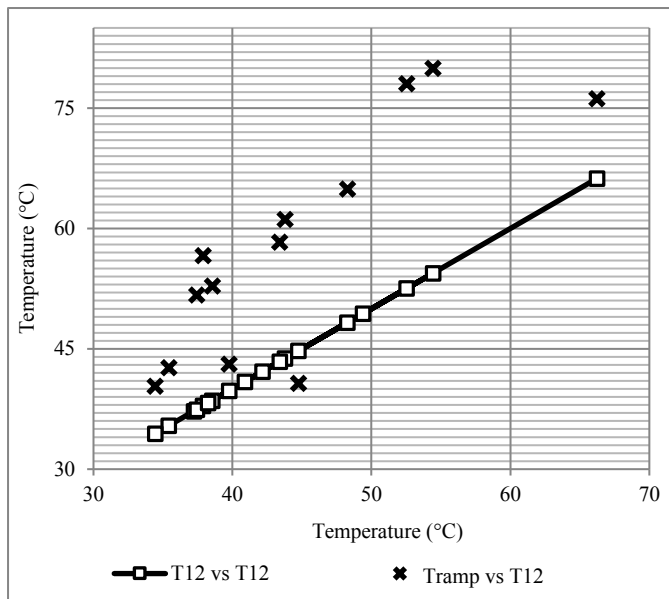


Fig. 5. Comparison between measurements taken in T12 and at the end of ramping during the slotting experiments

Fig. 6 shows the temperature ratio along the center line of the tool path (Tramp and T13 vs T12). On average, the 7° dive ramping angle leads to 20% lower gap between T12 and Tramp than 3° and 5° dive ramping angles. Higher axial feed per tooth is then advised to reduce the heat transfer into the workpiece subsurface during ramping.

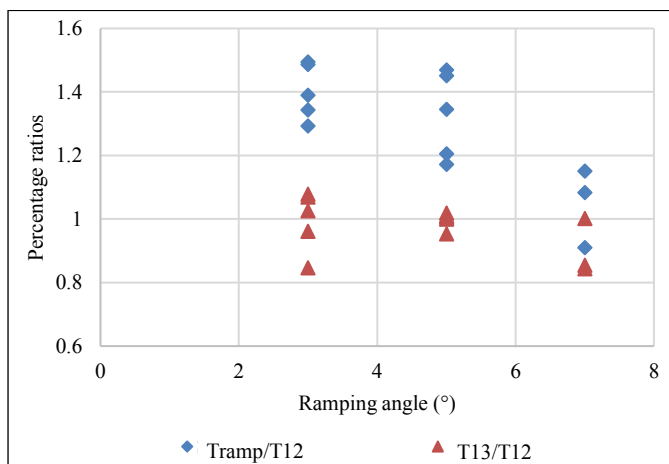


Fig. 6. Percentage ratio between Tramp/T12 and T13/T12 for different ramping angles

The temperature variations observed between the side and the center of the tool path (T12 vs T13) in slotting were between -15 % and +8% which shows a relative homogeneity of the temperature distribution in the width of the cut. No particular hot spot was identified in this regard.

It is worth noticing as well that the uncut chip thickness has a relatively significant impact on the heat generated along one edge pass. Higher temperatures tend to be observed close to the middle line, where the uncut chip is thicker and then the mechanical load on the edge is higher.

4. Conclusion

Chemical milling is on the verge to be replaced by mechanical milling partly due to environmental concerns. As opposed to the chemical milling, the mechanical milling generates heat during the cutting process which may lead to residual stresses after the heat dissipation. The combination of those stresses with the thin walls of some parts often leads to distorted components after machining. Therein, the influence of the cutting parameters (feed and speed) on the workpiece subsurface temperature has been investigated for the machining of 2024 aluminium alloy thin plates. In addition to the slotting process, the dive ramping impact is observed as well, considering different ramping angles. According to the results, lower workpiece subsurface temperatures are reached for high cutting speed and high feedrate. However, the feedrate has a greater impact on the temperature variations.

Regarding the ramping strategy, higher axial feed per tooth, which means higher ramping angle, is recommended to reduce heat generation. The feed deceleration in the slotting strategy due to the change of tool path direction leads to an increase of the temperature. The tool path generation is a point to be taken in the machining process as well. Smoother curves instead of sharp angular trajectories should be preferred to reduce the heat impact and then the residual stresses.

Further study would be interesting in developing analytical models that would be confirmed by those results.

References

- [1] C. L. Fu, C. K. Wang, T. G. Li, and W. S. Wang, "Simulation of End Milling for Weak-Rigidity Structural Parts of Aluminium Alloy in Aviation," *Advanced Manufacturing Systems*, vol. 201-203, pp. 332-336, 2011.
- [2] T. Ueda, A. Hosokawa, K. Oda, and K. Yamada, "Temperature on Flank Face of Cutting Tool in High Speed Milling," *CIRP Annals*, vol. 50, pp. 37-40, 2001.
- [3] N. A. Abukhshim, P. T. Mativenga, and M. A. Sheikh, "Heat generation and temperature prediction in metal cutting: A review and implications for high speed machining," *International Journal of Machine Tools and Manufacture*, vol. 46, pp. 782-800, 2006.
- [4] L. Zhu, S.-S. Peng, C.-L. Yin, T.-C. Jen, X. Cheng, and Y.-H. Yen, "Cutting temperature, tool wear, and tool life in heat-pipe-assisted end-milling operations," *The International Journal of Advanced Manufacturing Technology*, vol. 72, pp. 995-1007, 2014.
- [5] A. Braghini Junior, A. E. Diniz, and F. T. Filho, "Tool wear and tool life in end milling of 15-5 PH stainless steel under different cooling and lubrication conditions," *The International Journal of Advanced Manufacturing Technology*, vol. 43, pp. 756-764, 2008.
- [6] B. Bourouga, E. Guillot, B. Garnier, and L. Dubar, "Experimental study of thermal sliding contact parameters at interface seat of large strains," *International Journal of Material Forming*, vol. 3, pp. 821-824, 2010.
- [7] J. Z. Zhang, J. C. Chen, and E. D. Kirby, "Surface roughness optimization in an end-milling operation using the Taguchi design method," *Journal of Materials Processing Technology*, vol. 184, pp. 233-239, 2007.
- [8] J.-F. Chatelain, J.-F. Lalonde, and A. S. Tahan, "Effect of Residual Stresses Embedded within Workpieces on the Distortion of Parts after Machining," *International Journal of Mechanics*, vol. 6, pp. 43-51, 2012.
- [9] A. Il, J.-F. Chatelain, J.-F. Lalonde, M. Balazinski, and X. Rimpault, "An experimental investigation of the influence of cutting parameters on workpiece internal temperature during Al2024-T3 milling," *The International Journal of Advanced Manufacturing Technology*, 2018.
- [10] B. Davoodi and H. Hosseinzadeh, "A new method for heat measurement during high speed machining," *Measurement*, vol. 45, pp. 2135-2140, 2012.